

HIGH EFFICIENCY MONO-CRYSTALLINE SOLAR CELLS WITH SIMPLE MANUFACTURABLE TECHNOLOGY

Ajay Upadhyaya, Vijay Yelundur, Ajeet Rohatgi
Georgia Institute of Technology,
University Center of Excellence for Photovoltaics Research and Education
777 Atlantic Dr, Atlanta, GA 30332-250, USA

ABSTRACT: This paper describes the analysis and optimization of phosphorus-doped n^+ emitters for Si solar cells with screen-printed contacts to improve the uniformity of contact formation. Analysis of the simulated emitters showed that J_{oe} increases with the increase in phosphorus surface concentration. Cells fabricated on emitter having a higher surface concentration and shallower junction depth, were on an average 0.3% (absolute) higher in efficiency and 0.5 mA/cm² higher in J_{sc} values. Internal quantum efficiency analysis showed that the J_{sc} enhancement was due to better short wavelength response in these cells. In addition the fill factors were also slightly higher in the cells with higher surface concentration and shallower junction depth. SEM analysis showed larger (~1.5 μ m) and more uniformly distributed Ag crystallites on the surface of cells with emitter that had higher surface concentration. This may lead to a more tolerant contact firing process and result in a higher yield of high-efficiency cells. Furthermore, use of emitters with higher phosphorus surface concentration and shallower junction depth reduces the cell processing time appreciably leading to high throughput and cost savings in cell manufacturing. We were able to tailor the emitter profile and the firing conditions of a commercially available front silver paste to obtain good average FF's of 77.7% in conjunction with short circuit current (J_{sc}) of 34.8 mA/cm² and an open circuit (V_{oc}) of 619 mV and efficiency of ~17% on 149 cm² Czochralski silicon wafers.

Keywords: Diffusion, Contact, Cost reduction

1 INTRODUCTION

Screen-printing is the most widely used technology for the metallization of commercial crystalline silicon solar cells because it is fast, inexpensive, and can lead to high-efficiencies. However, commercial solar cells with screen-printed contacts typically have efficiencies lower than cells with evaporated or plated contacts, and exhibit significant more variability in fill factor and efficiency. These losses are due to the nature of the screen-printed contact interface with the emitter, which is composed of Ag crystallites that are in direct contact with the emitter and are separated from the bulk Ag gridline by an insulating glass layer. Thus the limiting carrier conduction mechanism in screen printed contacts is tunneling from the Ag crystallites through the glass layer to the Ag gridline. Schubert et al [1] and Hilali et al [2] have shown that uniform distribution of Ag crystallites and a thin glass layer are necessary to reduce contact resistance and achieve high fill factors. Additional losses in cells with screen printed contacts occur in the emitter layer that must be doped more heavily to reduce contact resistance. This leads to increased recombination in the emitter.

To overcome the resistance and recombination losses one needs a better understanding of the paste chemistry and its interaction with the emitter doping profile and the contact firing profile. Schubert has shown that a high phosphorus concentration near the emitter surface can enhance Ag crystallite formation [3], resulting in higher fill factors in cells with screen-printed contacts. Thus it appears that the fill factor in cells with screen-printed contacts can be improved by increasing the emitter doping near the surface. However the emitter doping profile must be carefully controlled because heavy doping ($>10^{19}$ cm⁻³) enhances Auger recombination, band gap narrowing, and a high surface recombination velocity (FSRV).

The aim of this study is to improve the performance and repeatability of the solar cells with screen-printed

contacts using an optimized emitter profile and contact firing. In this study we tailored the emitter profiles to reduce the emitter recombination and improve contact using a fixed emitter sheet resistance of 45 Ω/\square . We have used the combination of device and process simulations to narrow our optimization to two emitters formed in a tube furnace. The first emitter (Emitter-2) was relatively deep and had a relatively lower surface concentration. In order to reduce the junction depth of the emitter and increase the surface concentration, the other emitter (Emitter-3) profile was formed by reducing the process time and increasing the diffusion temperature.

2 APPROACH AND EXPERIMENT

2.1 Modeling and analysis of emitter profiles for cells with screen-printed contacts

Process and device modeling were performed to determine to what extent the phosphorus surface concentration could be increased, to enhance Ag crystallite formation, without significantly increasing heavy doping effects. It has been shown that a junction depth of ~0.5 μ m is desirable for cells with screen-printed contacts to avoid junction shunting during contact firing [4]. Phosphorus-doped n^+ emitter layers were simulated using SSUPREM3, a 1-dimensional process simulator by Silvaco International Inc. SSUPREM3 simulates the changes in a semiconductor's structure that result from the various processing steps used in its manufacture. The most important simulated results that can be obtained are (1) the layer thicknesses of the materials that make up the semiconductor structure and (2) the distribution of impurities within those layers and (3) the sheet resistivity of diffused regions in silicon layers. The emitter profiles that were simulated using SSUPREM3 are shown in Fig. 1.

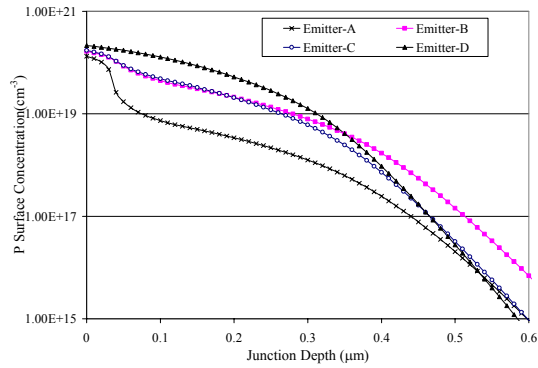


Figure 1 SSUPREM3 generated emitters

They all have a junction depth of $\sim 0.5\mu\text{m}$, which should be suitable for screen-printed contacts, with varying surface concentration from 1.32×10^{20} to $2.16 \times 10^{20} \text{ cm}^{-3}$. The emitter profiles in Fig. 1 were achieved by increasing the process temperature from T_A to T_D and decreasing the process time from t_A to t_D . To quantify the impact of the surface concentration on emitter recombination, the simulated profiles generated by SSUPREM3 were used as input to PC1D, a 1-dimensional solar cell device simulator. For each simulated emitter profile, the emitter saturation current density (J_{oe}) was calculated using PC1D for a fixed front surface recombination velocity (FSRV) of 30000 cm/s. Table 1 shows a summary of the characteristics of each emitter and the calculated J_{oe} . The results of the calculations show that J_{oe} increases from 138 fA/cm^2 to 285 fA/cm^2 when the surface concentration is increased from 1.32×10^{20} to $2.16 \times 10^{20} \text{ cm}^{-3}$. While Emitter-A has the lowest J_{oe} (138 fA/cm^2), this emitter is not compatible with high-volume cell manufacturing because the process time is very long ($t_A > 15$ hours). Emitter-D has the highest J_{oe} value and was eliminated from further consideration. Thus Emitter-B and C, which vary slightly in surface concentration and junction depth, were selected for further analysis.

Table I: Characteristics of emitter profiles simulated in SSUPREM3 and J_{oe} values calculated in PC1D.

Emitter Type	Diffusion Temperature	Diffusion Time	Junction Depth (μm)	P Surface Conc. (cm^{-3})	J_{oe} (fA/cm^2)
A	T_A	t_A	0.50	$1.32\text{E}+20$	138
B	T_B	t_B	0.56	$1.66\text{E}+20$	179
C	T_C	t_C	0.51	$1.72\text{E}+20$	185
D	T_D	t_D	0.50	$2.16\text{E}+20$	285

Note:- $T_A < T_B < T_C < T_D$ Note:- $t_A > t_B > t_C > t_D$

Emitter-B and Emitter-C were also simulated using PC1D to quantify the effect of the front surface recombination velocity (FSRV) on cell performance. For these simulations, a base resistivity of 1.3 ohm-cm, a lifetime of 150 μs and a back surface recombination velocity (BSRV) of 450 cm/s were used. As shown in Fig. 2 the J_{sc} of the Emitter-B is slightly lower ($\sim 0.2 \text{ mA/cm}^2$) than the J_{sc} of Emitter-C for all the FSRV's.

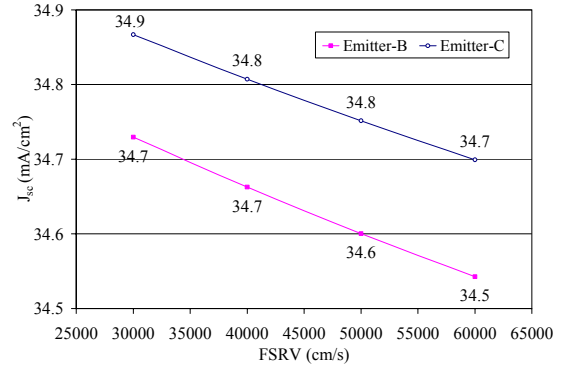


Figure 2 Effect of FSRV on J_{sc} for Emitter-B and Emitter-C.

This result shows that the emitter surface concentration can be increased from 1.66×10^{20} to $1.72 \times 10^{20} \text{ cm}^{-3}$ and the junction depth reduced from $0.56 \mu\text{m}$ to $0.51 \mu\text{m}$ to enhance J_{sc} . In addition to this enhancement, an increase in cell throughput is expected since $t_C < t_B$.

2.2 Experimental

Crystalline silicon solar cells were fabricated on commercially available large area (149 cm^2) p-type Czochralski (Cz) wafers to verify the enhancement in J_{sc} associated with Emitter-C that was demonstrated by device modeling. The wafers had a resistivity in the range of 0.5-1.7 ohm-cm and a thickness of 270 μm . An alkaline solution was used to form random pyramid surface texturing, followed by a modified RCA clean. Then two emitters (Emitter-2 and Emitter-3) were formed in a tube furnace using a liquid POCl_3 source. The temperature and time of the diffusion were varied to closely match the simulated profiles of Emitter-B (Emitter-2) and Emitter-C (Emitter-3) shown in Fig. 1. The diffusion temperature for Emitter-3 was higher than that for Emitter-2 and the total process time was shorter than that for Emitter-2. The sheet resistance, measured by the four-point probe method, for both Emitter-2 and Emitter-3 were in the range of 40-45 Ω/sq . After the measurement of the sheet resistance, edge isolation was performed by chemical etching followed by a brief chemical clean. Then an optimized single layer antireflection composed of low-frequency, direct PECVD silicon nitride with a thickness of 780-800Å and an index of refraction of 2.0 was deposited on the emitter surface. The back contact was composed of Al paste from Ferro Corp., used to form an Al-doped back surface field (Al-BSF) and Ag/Al paste for the rear bus bars.

A suitable moderately aggressive and commercially available Ag paste from Ferro Corp. was chosen to prevent junction shunting. We have found that this Ag paste has a wide firing window that should suit the contact firing on both the emitter profiles. Several solar cells were printed on both type of the emitters and co-fired in a belt furnace using the same firing profile. The lighted IV curve for each cell was measured after co-firing without any additional cell processing. Fig. 3 shows a process sequence used in this study to fabricate 149 cm^2 solar cells.

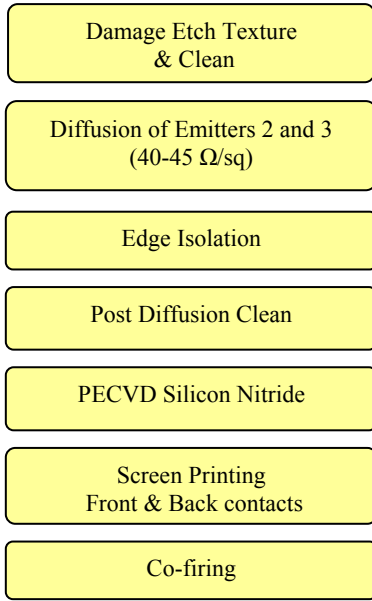


Figure 3: Process Sequence

3 RESULTS AND DISCUSSION

In order to confirm the actual surface concentration differences between the two emitters we performed SIMS analysis. The SIMS analysis was performed on similarly textured wafers and the profiles are shown in Fig. 4.

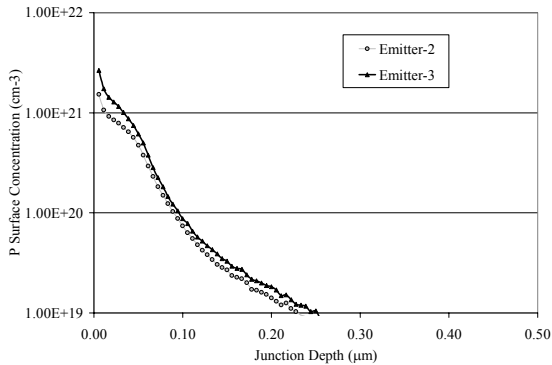


Figure 4: SIMS profile for Emitter-2 & 3

The surface concentration for Emitter-2 was $1.53 \times 10^{21} \text{ cm}^{-3}$ and $2.65 \times 10^{21} \text{ cm}^{-3}$ for Emitter-3. This trend is in agreement with the modeled data. It should be noted that the chemical phosphorous impurity profile is measured by SIMS while active phosphorous impurity profile generated by SSUPREM3 was used in this study.

The average IV data (measured at Georgia Tech) of several solar cells made on both Emitter-2 and Emitter-3 from one experiment is shown in Table II. The results show that the average efficiency of cells with Emitter-3 is 0.3% (absolute) higher than the cells with Emitter-2. In general, we find that the difference in absolute cell efficiency and J_{sc} are in the range of 0.1-0.3% and 0.3-0.5 mA/cm^2 . This efficiency difference is mainly caused by a difference in the average J_{sc} of cells from the two groups of cells, which is slightly larger than that predicted by

device modeling performed in Section 2. Table II shows the average efficiencies, however best cell efficiencies close to 17% were achieved on cells with Emitter-3.

Table II: Average IV data made on Emitter-2 and Emitter-3: - Area 149 cm^2

Emitter Type	V_{oc} (mV)	J_{sc} (mA/cm^2)	FF (%)	η (%)	R_s (ohm-cm^2)	R_{shunt} (ohm-cm^2)
2	619	34.3	77.1	16.4	1.13	34370
3	619	34.8	77.7	16.7	0.98	8094

To further analyze and understand this enhancement in J_{sc} , we measured the internal quantum efficiency (IQE) of representative cells with Emitters-2 and 3. The short wavelength IQE for the two cells is shown in Fig. 5. The results show that the IQE for the cell with Emitter-3 is superior up to 550 nm, after which the IQE values are indistinguishable.

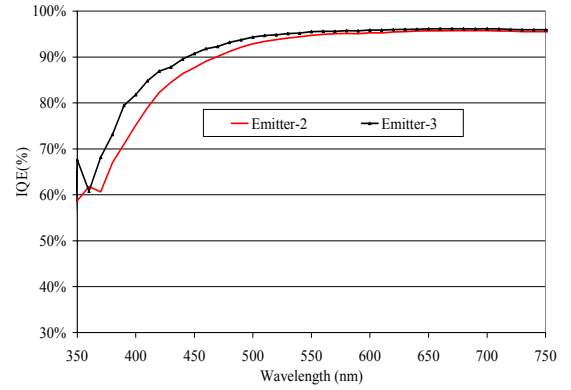


Figure 5: IQE on solar cells with Emitter-2 & 3

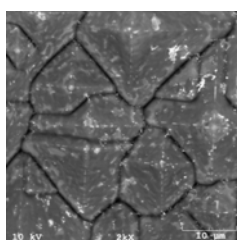
Further analysis of the quantum efficiency shows that the enhanced short wavelength response in the cell with Emitter-3 results in a gain of 0.4 mA/cm^2 in J_{sc} , which is in good agreement with the light I-V measurement for these cells, which is also shown in Table III. The enhanced short wavelength response in cells with Emitter-3 is attributed to a slightly shallower junction depth.

Table III: Measured J_{sc} comparison made on Emitter-2 and Emitter-3 with extracted J_{sc} : - Area 149 cm^2

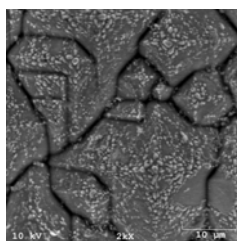
Emitter Type	J_{sc} from EQE (mA/cm^2)	J_{sc} Measured (mA/cm^2)
2	35.2	34.0
3	35.6	34.4
ΔJ_{sc}	0.4	0.4

The results in Table II also show that the average fill factor (FF) in cells with Emitter-3 is higher than that in cells with Emitter-2. This higher FF is associated with a lower series resistance (R_s) in cells with Emitter-3. To study this difference we performed SEM analysis on representative samples with both emitters. Before SEM analysis, the bulk Ag gridline and the glass layer were removed in dilute HF (5%) for 2 min. As shown in Fig. 6 (a) and (b) Ag crystallite formation in the case of

Emitter-3 is more uniformly distributed and larger in size compared to the Emitter-2, where crystallites appear mainly along the edges of pyramids. Fig. 7 shows that the Ag crystallites in the cell with Emitter-3 are $\sim 1.5 \mu\text{m}$ in size. The favorable crystallite size and distribution in the cell with Emitter-3 may lead to a more tolerant contact firing process, resulting in a higher yield of high-efficiency cells. The difference in Ag crystallite size and distribution that we observed may be caused by the difference in the phosphorus surface concentration between the two emitters. Schubert [3] has observed that Ag crystallite growth depends on the phosphorus concentration near the surface.



(a)



(b)

Figure 6: SEM micrographs of the top view of Ag crystallites under the Ag gridline of the cells with (a) Emitter-2, and (b) Emitter-3.

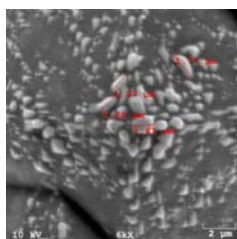


Figure: 7 SEM micrograph of top view of Ag crystallites under Ag gridline of the cells with Emitter-3 showing crystallite size of $\sim 1.5 \mu\text{m}$.

4 CONCLUSION

In this study emitter profiles suitable for solar cells with screen-printed contacts were designed and simulated in SSUPREM3. The emitters had junction depths of $0.5 \mu\text{m}$ to $0.6 \mu\text{m}$, to prevent junction shunting during contact firing, and phosphorus surface concentrations in the range of 1.32×10^{20} to $2.16 \times 10^{20} \text{ cm}^{-3}$, to improve Ag crystallite formation on the emitter and reduce series resistance. Analysis of the simulated emitters in PC1D showed that J_{oc} increases with the phosphorus surface concentration. Two simulated emitter profiles with similar sheet resistance values, but differing in process

time, process temperature, surface concentration and junction depth were prepared experimentally in a POCl_3 diffusion furnace and used for cell fabrication on 149 cm^2 Czochralski silicon wafers. Cells with the emitter having a higher surface concentration and shallower junction depth (Emitter-3) had 0.3% (absolute) higher efficiencies and 0.5 mA/cm^2 high J_{sc} values. This shows that a slight change in the emitter profile can appreciably alter the efficiency to have a significant impact on a 0.5-1.0 GW production line. Internal quantum efficiency analysis showed that the J_{sc} enhancement was due to better short wavelength response in cells with Emitter-3. Furthermore there is a slight enhancement in the fill factor of the cells of Emitter-3 because of higher density of Ag crystallites formation due to higher phosphorus surface concentration. SEM analysis after the removal of Ag bulk gridline and glass layer showed larger ($\sim 1.5 \mu\text{m}$) and more uniformly distributed Ag crystallites on the surface of Emitter-3. The favorable crystallite size and distribution in the cell with Emitter-3 may lead to a more tolerant contact firing process or a larger contact firing window and result in a higher yield with high-efficiency cells. In addition, use of Emitter-3 reduces the cell processing time appreciably leading to higher throughput and cost savings in cell manufacturing.

ACKNOWLEDGEMENTS

The authors would like to thank Roger Brennan at SOLECON labs for the spreading resistance measurements. The authors would also like to thank Bob Reedy at the NREL for the measurements of SIMS profiles.

4.3 References

- [1] Schubert et al. "Current Transport Mechanism in Printed Ag thick Film Contacts to an n-type Emitter of a Crystalline Si Solar Cell," 19th European Solar Energy Conference and Exhibition (2004).
- [2] Hilali et al, "Investigation of High-Efficiency Screen-Printed Textured Si Solar Cells with High Sheet Resistance Emitters," 31st IEEE Photovoltaic Specialists Conference (2005).
- [3] Schubert et al. "Silver Thick Film Contact Formation on Lowly Doped Emitters," 20th EC PVSEC, (2005).
- [4] S. Narasimha, PhD Thesis, Georgia Institute of Technology (2000) 121.